High-sensitivity optical biosensor based on cascaded Mach–Zehnder interferometer and ring resonator using Vernier effect

Xianxin Jiang, Yangqing Chen, Fang Yu, Longhua Tang, Mingyu Li, and Jian-Jun He*

State Key Laboratory of Modern Optical Instrumentation, Centre for Integrated Optoelectronics, Department of Optical Engineering Zhejiang University, Hangzhou 310027, China

**Corresponding author: jjhe@zju.edu.cn*

Received August 22, 2014; revised October 1, 2014; accepted October 5, 2014; posted October 7, 2014 (Doc. ID 221521); published November 3, 2014

We demonstrate an ultrahigh sensitivity silicon photonic biosensor based on cascaded Mach–Zehnder interferometer (MZI) and ring resonator with the Vernier effect using wavelength interrogation. Experimental results show that the sensitivities reached 2870 nm/RIU and 21,500 nm/RIU for MZI sensor and MZI-ring sensor, respectively. A biosensing application was demonstrated by monitoring the interaction between goat and antigoat immunoglobulin G (IgG) pairs. The measured results show that 1 ng/ml IgG resulted in 0.035 nm and 0.5 nm wavelength shift for MZI sensor and MZI-ring sensor, respectively. This high performance sensor is promising for medical diagnostic applications. © 2014 Optical Society of America

OCIS codes: (230.3120) Integrated optics devices; (130.6010) Sensors.
http://dx.doi.org/10.1364/OL.39.006363

Optical waveguide-based label-free biosensors have seen rapid development in the past few years because of their potential applications in many fields such as medical diagnosis, drug development, food quality control, environmental monitoring, and so on. Many high-performance waveguide sensors based on silicon-on-insulator (SOI) using configurations such as Mach–Zehnder interferometers (MZI) and ring resonators have been demonstrated owing to its advantages such as high sensitivity, high-density integration, and label-free detection [1–5]. However, traditional MZI sensors using intensity interrogation need highly sensitive power sensors and highly stable systems to achieve low noise level and high sensitivity. Although sensors based on ring resonators can overcome this problem because wavelength shift can be determined with high accuracies [2], a high-resolution spectrometer is required. In our previous work, we demonstrated that an architecture based on two cascaded ring resonators employing the Vernier effect was able to greatly improve the sensitivity [6–9], even by two orders of magnitude [8]. However, the extremely high sensitivity resulted from a very large Vernier amplification factor has a drawback because the envelope function of the total transmission spectrum of the double-ring is broad and it becomes difficult to determine the wavelength shift accurately, even with a curve fitting method [9]. An alternative sensing scheme based on frequency-resolved MZI was theoretically analyzed in [10]. Notte and Passaro also show theoretically that this sensing scheme can be developed for extremely high-sensitivity gas sensors [11].

In this Letter, we present an ultrahigh-sensitivity biosensor based on cascaded MZI and ring resonator with Vernier effect using wavelength interrogation. Experimental results show that sensitivities of 2870 and 21,500 nm/RIU are achieved for MZI sensor and MZI-ring sensor, respectively. By monitoring the binding reactions between goat and antigoat IgG pairs, we show that this sensor can detect extremely low concentration of IgG.

Figure 1(a) shows the optical microscope image of the cascaded MZI and ring resonator sensor. The sensor consists of a MZI cascaded with a ring resonator, in which the MZI is used for sensing while the ring resonator acts as a reference. The operation principle can be described as follows. The MZI has periodic transmission peaks that correspond to constructive interference when the phase difference between the sensing and reference arms is an integer multiple of 2π, which can be expressed as [10]:

$$\frac{2\pi}{\lambda}(L_s n_{\text{effs}} - L_r n_{\text{effr}}) = 2m\pi, \tag{1}$$

where λ is the operation wavelength and m is an integer, L_s, L_r and n_{effs}, n_{effr} are the lengths, effective indices of the sensing arm, and reference arm, respectively. This

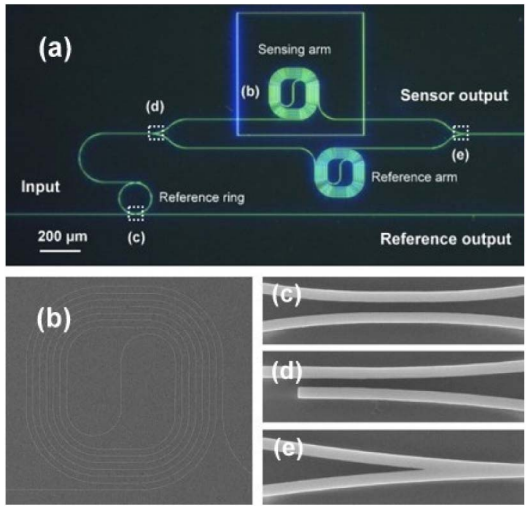

Fig. 1. Optical microscope image of the cascaded MZI and ring resonator sensor (a), the SEM images of the sensing waveguide (b), the directional coupler for ring-waveguide coupling (c), the directional coupler-based unequal-power splitter of the MZI (d), and the Y-junction power combiner of the MZI (e).

 © 2014 Optical Society of America

equation is quite similar to the resonant condition of a ring resonator. Therefore, the sensitivity defined as the wavelength shift $\Delta\lambda$ caused by a change of refractive index in the sensing arm of the MZI is given by:

$$\Delta\lambda = \frac{\lambda L_s \Delta n_{\text{effs}}}{L_s n_{gs} - L_r n_{gr}}, \tag{2}$$

where Δn_{effs} is the change of effective index in the sensing arm, n_{gs}, n_{gr} are the group indices of sensing and reference arm, respectively. We define M as the length ratio between the sensing arm and the reference arm, that is $M = L_s/L_r$, then $\Delta\lambda$ can be written as $\Delta\lambda = \lambda M \Delta n_{\text{effs}}/(M n_{gs} - n_{gr})$. It is obvious that the sensitivity of MZI sensor using wavelength interrogation can be much higher than that of a ring resonator-based sensor, which is given by $\Delta\lambda = \lambda \Delta n_{\text{effs}}/n_{gs}$, if an appropriate M is chosen so that the denominator is small. The free spectral range (FSR) defined as the wavelength spacing between two transmission maxima is given by $\text{FSR}_{\text{MZI}} = \lambda^2/L_r(M n_{gs} - n_{gr})$. The cascading of MZI with a ring resonator results in a series of transmission peaks with periodic envelope function. Using the cascaded MZI-ring, the wavelength shift of the MZI is translated into a much larger shift of the total transmission envelope function due to the Vernier effect. The wavelength shift is given by $F\Delta\lambda$, with the Vernier amplification factor $F = \text{FSR}_{\text{ring}}/|\text{FSR}_{\text{ring}} - \text{FSR}_{\text{MZI}}|$, where FSR_{ring} is the FSR of the reference ring [6]. While this Vernier amplification is similar to the case of cascaded double-ring sensors [6,7], for a given Vernier amplification factor F, the sensitivity of the MZI-ring can be much higher because the wavelength shift of the MZI is larger than that of a single ring by a factor of $M n_{gs}/(M n_{gs} - n_{gr})$.

The MZI-ring sensor chips were fabricated on an SOI wafer with a 250-nm silicon top layer and 3-μm buried oxide. Waveguides of 500 nm width were patterned by electron-beam lithography using a ma-N 2403 photoresist and etched through the silicon layer in an inductively coupled plasma (ICP) reactive ion-etching (RIE) systems using C_4F_8/SF_6 gases. The wafer was then immersed in a solution consisting of H_2O_2 and H_2SO_4 at a ratio of 1:1 for 10 minutes to form a thin layer of SiO_2 for later surface functionalization and to reduce the waveguide loss. SEM images of the spiral sensing waveguides, the directional coupler of the reference ring, the directional coupler splitter, and the Y-junction combiner of the MZI are shown in Figs. 1(b), 1(c), 1(d) and 1(e), respectively. The sensing arm with a length of 5 mm is incorporated in an area of 250 μm × 250 μm by using the spiral waveguide. A direction coupler of 4 μm length with a gap of 0.4 μm resulting in a splitting ratio of 20%:80% and a symmetric Y-junction combiner were used for the MZI to achieve the best performance as the loss was measured to be about 3 and 12 dB/cm for waveguides with SU8 upper cladding layer and water upper cladding layer, respectively. After the waveguide fabrication, the wafer was covered with a 1.8-μm SU8 polymer, and a window was opened upon the sensing arm by standard UV lithography with a 2-min oxygen plasma treatment, as shown in Fig. 1(a). A microfluidic channel made of polydimethylsiloxane (PDMS) was integrated on the wafer to provide the advective transport of analyte.

We first characterized a sensor based on MZI alone, in which both the sensing and reference arms were 5150 μm in length, corresponding to $M = 1$. A tunable laser and a power sensor were used to measure the sensor response. Fully etched-focused grating couplers with 890 nm period, 68% duty cycle were used for highly efficient and stable coupling of TM mode into and out of the chip. Solutions were delivered into the microfluidic channel using a syringe pump. Fig. 2(a) shows the transmission spectrum of the MZI sensor when deionized water was delivered. The group indices for the sensing and reference waveguides were measured to be 4.189 and 4.443, respectively, at 1560 nm wavelength. Aqueous solutions of NaCl with an increasing concentration in steps of 0.05%, corresponding to a refractive index change of 9×10^{-5} were used to measure the sensor response, which is shown in Fig. 2(b). The sensitivity as measured by the slope of the curve reached 1960 nm/RIU, more than an order of magnitude higher compared to that of the sensor based on a single ring resonator [1].

We also investigated the sensitivity as a function of waveguide length ratio between the sensing arm and the reference arm, corresponding to the value M. We designed MZI sensors with different sensing arm lengths of 5020, 5280, 5400 μm with the same reference arm length of 5150 μm as described above, corresponding to the M value of 0.975, 1.025, and 1.05, respectively. The measured sensitivities were 2870, 1350, and 980 nm/RIU, respectively. Both theoretical simulation and the experimental results are shown in Fig. 3.

For the cascaded MZI and ring resonator sensor, the lengths of the sensing arm and the reference arm are

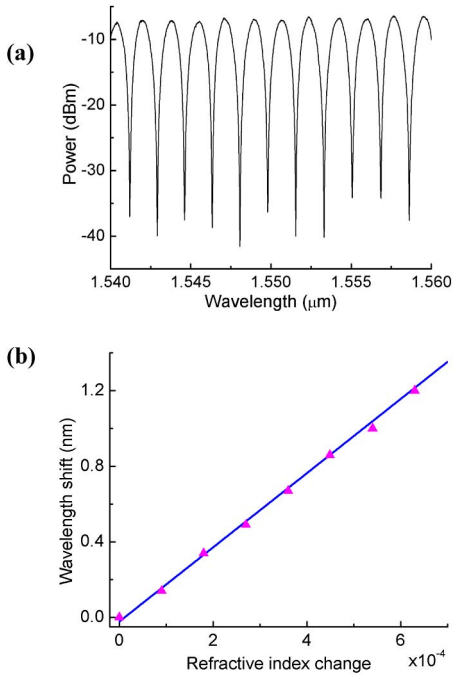

Fig. 2. (a) Measured transmission spectrum of sensor based on MZI alone and (b) measured wavelength shift versus refractive index change of aqueous solutions of NaCl with different concentrations.

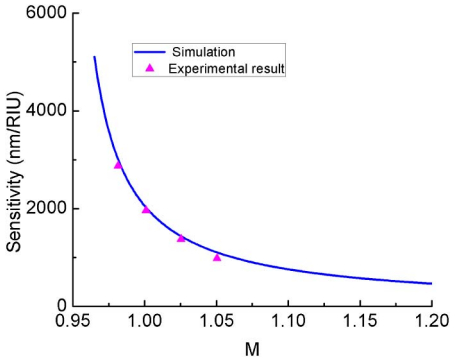

Fig. 3. Sensitivity versus the length ratio between the sensing arm and the reference arm.

5400 and 5150 μm, corresponding to $M = 1.05$ and $FSR_{MZI} = 0.991$ nm. The perimeter of the reference ring is 560 μm, corresponding to FSR_{ring} of 1.04 nm. The FSR difference is 4.67%, resulting in a Vernier amplification factor of 21. The measured transmission spectrum of the MZI-ring sensor is shown in Fig. 4(a). The sensitivities were also measured as previously described and the results are shown Fig. 4(b). The slopes of the curves are 980 and 21,500 nm/RIU for MZI sensor and MZI-ring sensor, respectively. It should be noted that the sensitivity is comparable to the previously reported 24,300 nm/RIU for the sensor based on cascaded double-ring sensor [8], while a much lower Vernier amplification factor of 21 is used here as compared to the previously reported 150. The lower Vernier amplification factor corresponds to a narrower peak in the envelope function and thus a higher peak detection accuracy.

To demonstrate the biosensing applications, we used the sensor to monitor the interaction between goat and antigoat immunoglobulin G (IgG) pairs. The standard silicon surface functionalization procedure was applied on the fabricated sensor [12,13]. The sensor chip was first silanized with 3-Aminopropyltriethoxysilane (APTES) and rinsed with ethanol. Then it was immersed in glutaraldehyde solution for further preparation and rinsed by 0.01 M phosphate buffer solution (PBS) with PH 7.4. The APTES/glutaraldehyde procedure was used because it offers an effective covalent attachment of streptavidin to the SiO_2 surface [14]. Then the modified sensor was exposed to 0.1 mg/ml streptavidin, followed by 0.5 mg/ml bovine serum albumin (BSA) to block unoccupied sites, and PBS was used to remove redundant BSA molecules. Finally the functionalized sensor was immersed in 0.1 mg/ml biotinylated goat IgG for deposition of receptor molecules, followed by a PBS rinse. Then a PDMS microfluidic channel was mounted on the sensor to deliver antigoat IgG solutions with concentrations of 1, 10, 50 ng/ml, separated by PBS buffers. Besides, a thermoelectric cooler (TEC) was used to maintain the sensor at a constant temperature of 25°C during the measurement. The measured sensor response is shown in Fig. 5. The wavelength shifts for 1, 10, 50 ng/ml antigoat IgG are about 0.035, 0.18, 0.35 nm, respectively, for the MZI sensor, and 0.5, 2.5, 4.1 nm, respectively, for the MZI-ring sensor. While the wavelength shift of the MZI-ring sensor is about 14 times larger than that of the MZI sensor, the wavelength measurement error also increased due to the peak broadening in the envelope function. The estimated lowest detectable concentration for the MZI sensor is about 0.29 ng/ml IgG with a minimal detectable wavelength shift of 10 pm. For the MZI-ring sensor, the reliable minimal detectable wavelength shift is around 50 pm using data fitting, which gives the lowest detectable concentration of 0.1 ng/ml IgG. That is, while the spectral resolution requirement of the measurement instrument can be relaxed by about 5 times, the effective sensitivity of the MZI-ring sensor in this device example is still about three times higher than that of the MZI sensor. This can be further improved by increasing the Vernier amplification factor. The achieved sensitivity is more than an order

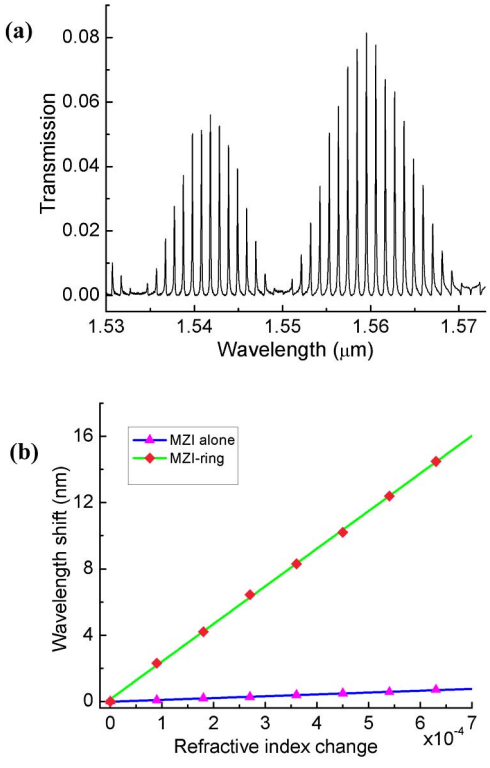

Fig. 4. (a) Measured transmission spectrum of the MZI-ring sensor and (b) measured wavelength shift versus refractive index change of aqueous solutions of NaCl with different concentrations.

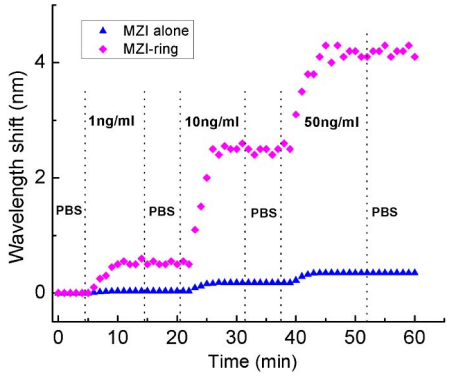

Fig. 5. Wavelength shift of the sensors in response to continuous injection of antigoat IgG with concentrations of 1 ng/ml, 10 ng/ml, 50 ng/ml, and PBS buffer.

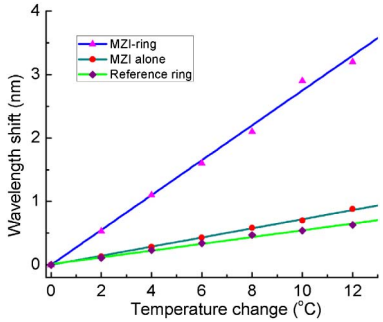

Fig. 6. Wavelength shift versus temperature change for reference ring, MZI alone, and MZI-ring.

of magnitude higher compared to those achieved by sensors based on traditional MZI [4], and also much higher than that of the most advanced commercial biosensors developed by Genalyte Inc. [2,15].

The temperature dependence of the sensors has also been investigated. The TEC was used to heat the sensor from 20°C to 32°C, and the wavelength shifts versus temperature change are shown in Fig. 6. The measured wavelength shifts change linearly with temperature with slopes of 58, 76, 271 pm/°C for the reference ring, MZI sensor and MZI-ring sensor, respectively. In principle, the temperature drift for MZI can be completely eliminated by appropriately designing the length difference between its two arms because it is mainly caused by the mismatch of thermo-optic coefficients between the waveguides cladded by SU8 and the waveguide cladded by water solutions, at the expense of some sensitivity degradation. Since the temperature drift for cascaded MZI-ring is determined by both the temperature drift of the individual elements and their differences, tradeoffs have been taken in choosing the design parameters used here. Considering the high sensitivities, these temperature drifts are acceptable for typical applications, while temperature stability using TEC control is always necessary in extremely low concentration detection situations.

In conclusion, we have experimentally demonstrated a highly sensitive biosensor based on cascaded MZI with ring resonator using wavelength interrogation. The sensitivities reached 2870 nm/RIU for MZI sensor and 21,500 nm/RIU for cascaded MZI-ring sensor. A biosensing application was demonstrated by monitoring the interaction between goat and antigoat immunoglobulin G (IgG) pairs. The measured results show that 1 ng/ml IgG resulted in 0.035 and 0.5 nm wavelength shifts for MZI sensor and MZI-ring sensor, respectively. The temperature drift was also measured to be 76 and 271 pm/°C for the sensors based on MZI alone and MZI-ring, respectively. This high sensitivity sensor is promising for medical diagnosis and other applications.

This work was supported by National High Technology Research and Development Program of China (No. 2014AA06A504), Fundamental Research Funds for Central Universities (No. 2014QNA5018), and by Zhejiang Provincial Key Laboratory for Sensing Technologies.

References

1. K. De Vos, I. Bartolozzi, E. Schacht, P. Bienstman, and R. Baets, Opt. Express **15**, 7610 (2007).
2. A. L. Washburn, M. S. Luchansky, A. L. Bowman, and R. C. Baily, J. Anal. Chem. **82**, 69 (2010).
3. C. F. Carlborg, K. B. Gylfason, A. Kaźmierczak, F. Dortu, M. J. Banuls Polo, A. M. Catala, G. M. Kresbach, H. Sohlstrom, T. Moh, L. Vivien, J. Popplewell, G. Ronan, C. A. Barrios, G. Stemme, and W. van der Wijngaart, Lab Chip **10**, 281 (2010).
4. D.-X. Xu, M. Vachon, A. Densmore, R. Ma, A. Delâge, S. Janz, J. Lapointe, Y. Li, G. Lopinski, D. Zhang, Q. Y. Liu, P. Cheben, and J. H. Schimid, Opt. Lett. **35**, 2771 (2010).
5. A. Densmore, M. Vachon, D.-X. Xu, S. Janz, R. Ma, Y.-H. Li, G. Lopinski, A. Delâge, J. Lapointe, C. C. Luebbert, Q. Y. Liu, P. Cheben, and J. H. Schimid, Opt. Lett. **34**, 3598 (2009).
6. L. Jin, M. Li, and J.-J. He, Opt. Commun. **284**, 156 (2011).
7. L. Jin, M. Li, and J.-J. He, Opt. Lett. **36**, 1128 (2011).
8. X. Jiang, J. Ye, J. Zou, M. Li, and J.-J. He, Opt. Lett. **38**, 1349 (2013).
9. T. Claes, W. Bogaerts, and P. Bienstman, Opt. Express **18**, 22747 (2010).
10. M. Kitsara, K. Misiakos, I. Raptis, and E. Makarona, Opt. Express **18**, 8193 (2010).
11. M. L. Notte and V. M. N. Passaro, Sens. Actuators B **176**, 994 (2013).
12. K. Schmitt, B. Schirmer, C. Hoffmann, A. Brandenburg, and P. Meyrueis, Biosens. Bioelectron. **22**, 2591 (2007).
13. N. Trummer, N. Adányi, M. Váradi, and I. Szendrö, Fresenius J. Anal. Chem. **371**, 21 (2001).
14. I. Migneault, C. Dartiguenave, M. J. Bertrand, and K. C. Waldron, BioTechniques **37**, 790 (2004).
15. Genalyte. Inc, http://www.genalyte.com.